Cyclin-Dependent Kinase Inhibitor 2b Mediates Excitotoxicity-Induced Death of Retinal Ganglion Cells

Hiroshi Tawarayama,[1,2] Qiwei Feng,[1] Namie Murayama,[1] Noriyuki Suzuki,[1] and Toru Nakazawa[1–3]

[1]Department of Ophthalmology, Tohoku University Graduate School of Medicine, Sendai, Japan
[2]Division of Retinal Disease Control, Tohoku University Graduate School of Medicine, Sendai, Japan
[3]Division of Advanced Ophthalmic Medicine, Tohoku University Graduate School of Medicine, Sendai, Japan

Correspondence: Toru Nakazawa; Department of Ophthalmology, Tohoku University Graduate School of Medicine, 1-1 Seiryo-machi, Aoba-ku, Sendai 980-8574, Japan; ntoru@oph.med.tohoku.ac.jp.

HT and QF contributed equally to this work.

Submitted: May 16, 2019
Accepted: October 3, 2019

Citation: Tawarayama H, Feng Q, Murayama N, Suzuki N, Nakazawa T. Cyclin-dependent kinase inhibitor 2b mediates excitotoxicity-induced death of retinal ganglion cells. *Invest Ophthalmol Vis Sci*. 2019;60:4479–4488. https://doi.org/10.1167/iovs.19-27396

Purpose. Glutamate excitotoxicity seems to contribute to retinal ganglion cell (RGC) death in various eye diseases, but the underlying molecular mechanisms are not fully understood. We studied the roles of cyclin-dependent kinase inhibitors Cdkn2a and Cdkn2b, known as cellular stress-related senescence markers, in *N*-methyl-d-aspartate (NMDA)-induced RGC death.

Methods. Gene expression was analyzed using quantitative reverse transcription (qRT)-PCR, in situ hybridization, and immunochemistry. Cdkn2a and Cdkn2b gain- and loss-of-function experiments were performed using the adeno-associated virus type 2 (AAV2)-mediated gene delivery system. AAV2-CRISPR-Cas9–mediated knockout of Cdkn2a or Cdkn2b was validated using cultured cells by T7 endonuclease I assay and Western blot analysis. The effects of altered expression of Cdkn2a and Cdkn2b on NMDA-induced RGC death were evaluated by quantification of RNA binding protein with multiple splicing (Rbpms)-immunoreactive RGCs.

Results. Intravitreal NMDA injection resulted in upregulation of Cdkn2a and Cdkn2b expression in RGCs of the mouse retina. AAV2-mediated overexpression of Cdkn2b led to increased expression of Cdkn2a in RGCs, but not vice versa. Overexpression of Cdkn2b, but not Cdkn2a, resulted in a further reduction in RGC viability in NMDA-injected retinas. However, excessive levels of Cdkn2a or Cdkn2b had no effect on RGC viability in healthy mice. AAV2-CRISPR-Cas9–mediated knockout of either Cdkn2a or Cdkn2b attenuated NMDA-induced RGC death.

Conclusions. Cdkn2a and Cdkn2b have pivotal roles in the regulation of excitotoxic RGC degeneration under NMDA-induced pathologic conditions. Our findings imply that Cdkn2a and Cdkn2b are novel therapeutic targets for ocular diseases displaying excitotoxicity-induced neuronal degeneration.

Keywords: neuroexcitotoxicity, NMDA model, RGC death, Cdkn2a, Cdkn2b

Retinal ganglion cell (RGC) death is an irreversible symptom observed in eye diseases, including ischemia-reperfusion injury, diabetic retinopathy, and glaucoma, leading to visual impairment and blindness. According to animal experimental models, neuronal degeneration in these diseases is attributable at least partly to glutamate receptor-mediated excitotoxic neuronal cell death.[1–8] Ischemia-reperfusion injury leads to RGC loss,[9–11] which is attenuated by treatment with glutamate-receptor antagonists.[12–14] Excitatory neurotransmitter-induced toxicity is a pathomechanism of RGC degeneration in the hyper- and normal-tension glaucoma. Administration of the *N*-methyl-D-aspartate (NMDA) receptor antagonist memantine prevents RGC loss in animal models of glaucoma.[4,15,16] Therefore, molecular events leading to glutamate-induced RGC death must be clarified to prevent RGC loss in eye diseases associated with neuronal excitotoxicity.

Cyclin-dependent kinase inhibitors Cdkn2a and Cdkn2b (also known as $p16^{INK4a}$ and $p15^{INK4b}$, respectively) inhibit the activity of cyclin-dependent kinases (Cdks) 4 and 6,[17–19] which cooperate with D-type cyclins to activate retinoblastoma family proteins, and consequently regulate cell cycle progression.[20,21] Primary cells derived from normal tissues undergo irreversible cell cycle arrest, known as senescence, after a limited number of cell divisions. Overexpression of Cdkn2a or Cdkn2b results in senescence transition in established cell lines,[22] and Cdkn2a expression is upregulated in aged cultured cells and tissues.[23–25] The effect of altered Cdkn2a expression on RGC survival has been investigated using animal models of glaucoma. In mice with ocular hypertension, retinal Cdkn2a expression was upregulated and senescence-associated beta-galactosidase (SA-ß-gal)–positive cell number increased in the retinal ganglion cell layer (GCL).[26] High IOP resulted in reduced RGC numbers; however, *Cdkn2a* deficiency rescued the RGC loss.[26,27] The human *CDKN2B-AS* gene,located within the *CDKN2B-CDKN2A* gene cluster, encodes a noncoding RNA that regulates the expression of neighboring genes by interacting with polycomb proteins.[28] Single-nucleotide polymorphisms in the *CDKN2B-AS* locus are associated with human glaucoma.[29–31] Partial deletion of the *CDKN2B-AS* locus in mice led to increased *Cdkn2a* mRNA expression in the optic nerve.[32] Furthermore, *CDKN2B-AS* mutant mice displayed increased RGC vulnerability to microbead-mediated ocular hypertension, leading to fewer surviving RGCs.[32] These findings implicated that Cdkn2a is a key regulator of RGC death in pathologic conditions; however, little is known about the role of Cdkn2b in RGC death induction.

Copyright 2019 The Authors

This work is licensed under a Creative Commons Attribution-NonCommercial-NoDerivatives 4.0 International License.

Downloaded from abstracts.iovs.org on 04/23/2024

Glutamate excitotoxicity seems to contribute to RGC death in various eye diseases.[1–8] However, the underlying molecular mechanisms are not fully understood. We elucidated the roles of Cdkn2b and Cdkn2a in NMDA receptor-related RGC death using an animal experimental model established by intravitreal NMDA injection.[33,34]

Materials and Methods

Animals

Eight- to 12-week-old male C57BL/6J mice were obtained from SLC (Shizuoka, Japan) or CLEA (Tokyo, Japan) and were maintained at animal facilities in Tohoku University Graduate School of Medicine under a 12-hour light/dark cycle. All animal experiments and animal care were conducted according to procedures and guidelines approved by the committee on animal research at Tohoku University, and the ARVO Statement for the Use of Animals in Ophthalmic and Vision Research.

NMDA Administration

Mice were anesthetized by intraperitoneal injection of sodium pentobarbital dissolved in normal saline (78 mg/kg body weight), and then administered with 10 nmol NMDA (Sigma-Aldrich Corp., St. Louis, MO, USA) dissolved in PBS (2 μL 5 mM NMDA solution per eye) intravitreally using a microsyringe with a sharp 32-gauge needle (Ito, Shizuoka, Japan).

Quantitative Reverse-Transcription (qRT)-PCR

Total RNA was extracted from mouse retinas using the miRNeasy Mini Kit (Qiagen, Hilden, Germany) and reverse-transcribed into cDNA using the SuperScript III First-Strand Synthesis System (Thermo Fisher Scientific, Waltham, MA, USA). qRT-PCRs were run in a 7500 Fast Real-Time PCR System (Thermo Fisher Scientific) using TaqMan Fast Universal PCR Master Mix (Thermo Fisher Scientific) and a mixture of predesigned TaqMan primers and probes (Thermo Fisher Scientific or Integrated DNA Technologies; Supplementary Table S1).

AAV Plasmid Construction

Cdkn2a and Cdkn2b expression plasmids were constructed by ligating hemagglutinin (HA) tagged-DNA fragments containing the entire coding region of mouse *Cdkn2a* (NM_001040654: 82–588) or *Cdkn2b* (NM_007670: 236–628), amplified from cDNA prepared from adult mouse retina using KOD DNA polymerase (Toyobo, Osaka, Japan), into a mammalian expression vector (Cell Biolabs, San Diego, CA) containing the adeno-associated virus (AAV) inverted terminal repeat, cytomegalovirus (CMV) promoter, internal ribosome entry site (IRES), and green fluorescent protein gene (*gfp*; pAAV-CMV-*Cdkn2a*-IRES-GFP or pAAV-CMV-*Cdkn2b*-IRES-GFP). For clustered regularly interspaced short palindromic repeats (CRISPR)/CRISPR-associated protein 9 (Cas9)-mediated loss-of-function assays of *Cdkn2a* and *Cdkn2b*, single-guide (sg)RNAs were designed at the 208th and 353rd nucleotide of mouse *Cdkn2a* (NM_001040654) or *Cdkn2b* (NM_007670) in the reverse strand, using an online tool (CRISPOR; available in the public domain at http://crispor.tefor.net/), and ligated into the *Bsa*I restriction recognition site of pX601-AAV-CMV::NLS-SaCas9-NLS-3xHA-bGHpA;U6::BsaI-sgRNA (pX601; a gift from Feng Zhang; Addgene plasmid #61591).[35] Sequences of the constructed plasmids were confirmed by Sanger sequencing. Information on the oligos used for plasmid construction is shown in Supplementary Table S2.

AAV2 Production and Administration

Production of AAV2 for intravitreal injection and determination of AAV2 vector genome titers were conducted as reported previously.[36] To infect RGCs with exogenous protein-encoding AAV2, ten billion genome copies of AAV2 were injected with 2.0 μL Ca^{2+} and Mg^{2+}-free PBS (Nacalai Tesque, Kyoto, Japan) into the vitreous humor of mice anesthetized with a mixture of ketamine (180 mg/kg) and xylazine (90 mg/kg).

In Situ Hybridization (ISH)

Dissected eyes were fixed with 4% paraformaldehyde dissolved in PBS (4% PFA/PBS) at 4°C overnight, incubated in 20% sucrose in PBS at 4°C overnight, and embedded in O.C.T. compound (Sakura Finetek Japan, Tokyo, Japan). The eyes were sliced at 10-μm thickness using a cryostat (Leica, Wetzlar, Germany). Retinal sections containing the optic nerve head were collected and used in following experiments. To prepare complementary RNA probes, mouse *Cdkn2a* (NM_001040654.1: bases 82-585) and *Cdkn2b* (NM_007670.4: bases 236-625) were amplified by PCR using primers containing the T3 or T7 promoter sequence (Supplementary Table S2), and pAAV-CMV-*Cdkn2a*-IRES-GFP or pAAV-CMV-*Cdkn2b*-IRES-GFP as templates. Amplicons were purified using the NucleoSpin Gel and PCR Clean-up Kit (Macherey-Nagel, Düren, Germany). Purified DNA fragments were used to synthesize digoxigenin-labeled antisense probes for mouse *Cdkn2a* and *Cdkn2b*. ISH was conducted as reported.[37]

Immunohistochemistry

Dissected retinas were fixed with 4% PFA/PBS at 4°C overnight. After washing, the retinas were incubated in radioimmunoprecipitation assay (RIPA) buffer for 4 hours, and then incubated with 10% normal donkey serum in PBS containing 0.1% Tween-20 (PBST) for 1 hour at room temperature to block nonspecific antibody binding. The specimens were incubated with primary antibodies at 4°C under shaking for 3 days. After extensive washing, the specimens were incubated with appropriate fluorophore-conjugated secondary antibodies. Retinal sections were prepared as described above. After blocking with 10% normal donkey serum in PBST, retinal sections were treated with primary antibodies at 4°C overnight, and then treated with secondary antibodies at room temperature for 2 hours. Antibodies used for immunohistochemistry are listed in Supplementary Table S3.

Cell Culture

NIH3T3-L1 cells (JCRB, Osaka, Japan) were maintained in Dulbecco's modified Eagle's medium (DMEM; Thermo Fisher Scientific) supplemented with 10% fetal bovine serum (Cosmo Bio), and were subcultured upon reaching 80% confluency.

Plasmid Transfection and Sorting of Transfectants

NIH3T3-L1 cells were seeded into 6-well cell culture plates, incubated for 1 day, and then transfected with the CRISPR-Cas9 plasmids using Avalanche-Everyday Transfection Reagent (EZ Biosystems, College Park, MD) according to the manufacturers' instructions. On the third day after transfection, cells were harvested in 0.25% trypsin-EDTA solution (Thermo Fisher Scientific) and sorted by fluorescence-activated cell sorting (FACS) on a FACSAria III (BD Biosciences, Franklin Lakes, NJ, USA) to obtain GFP-expressing transfectants. Separated cells

Investigative Ophthalmology & Visual Science

Downloaded from abstracts.iovs.org on 04/23/2024

were used in T7 endonuclease I (T7E1) assays and Western blot analysis.

T7E1 Assay

Genomic DNA was purified from FACS-sorted bulk transfectants using the QIAamp DNA Mini Kit (Qiagen) according to the manufacturer's instructions. Genomic regions containing CRISPR-Cas9 targets were amplified using KOD DNA polymerase (Toyobo) with *Cdkn2a*- and *Cdkn2b*-specific primers (Supplementary Table S2). After purification with the NucleoSpin Gel and PCR Clean-up Kit (Macherey-Nagel, Düren, Germany), PCR products were denatured at 95°C for 5 minutes, and then reannealed by decreasing the temperature gradually from 95°C to 60°C. Reannealed DNA fragments were treated with T7E1 (New England Biolabs, Ipswich, MA) at 37°C for 30 minutes, and then electrophoresed on 1.5% agarose gels.

Western Blotting

FACS-sorted single transfectants were harvested after expansion and sonicated using a Bioruptor UCD-300 (Cosmo Bio, Tokyo, Japan) in RIPA buffer containing protease inhibitor cocktail (Cayman Chemical, Ann Arbor, MI, USA). Sonicated cells were centrifuged to obtain lysates, and protein concentrations were determined using the Pierce BCA Protein Assay Kit (Thermo Fisher Scientific). Total protein (30–50 μg) was analyzed by Western blotting according to routine protocols. Antibodies used for Western blotting are listed in Supplementary Table S3.

Image Acquisition

Images were captured using a BZ-9000 fluorescence microscope (Keyence, Osaka, Japan). Contrast and brightness adjustment and photo trimming were performed in Adobe Photoshop Elements (Adobe Systems, San Jose, CA, USA).

Quantification of RNA Binding Protein With Multiple Splicing (Rbpms)-Immunopositive RGCs

Images were captured with a ×20 objective lens at different microscopic fields near the optic nerve head of each flat-mounted retina immunostained for Rbpms. $Rbpms^+$ cells in each image were counted using ImageJ software (National Institutes of Health, Bethesda, MD, USA) and expressed as the number of RGCs per mm^2. The average was calculated from images obtained from the same retina, and for five to eight retinas per experimental group.

Statistics

Quantitative data were analyzed using Student's *t*-test for two experimental groups or ANOVA followed by Tukey-Kramer post hoc tests for more than two experimental groups, using JMP Pro 14 software (SAS Institute, Cary, NC, USA). $P < 0.05$ was considered significant.

Results

Intravitreal NMDA Injection Alters *Cdkn2a* and *Cdkn2b* Gene Expression in RGCs

We first investigated the effects of intravitreal NMDA injection (10 nmol per eye) on the expression of *Cdkn2a* and *Cdkn2b*, as well as the RGC marker *Rbpms*, in the mouse retina by qRT-PCR. Retinas were collected at 10, 20, and 30 hours after injection. *Rbpms* mRNA expression was unchanged at 10 hours, but significantly decreased at 20 and 30 hours, suggesting that RGCs underwent NMDA-induced cell death 20 hours after injection (Fig. 1A). Retinal *Cdkn2b* mRNA was upregulated at 20 hours (Fig. 1A). Thus, the timing of *Cdkn2b* mRNA upregulation coincided with the reduction in *Rbpms* mRNA. *Cdkn2b* mRNA expression further increased at 30 hours (Fig. 1A). The expression level of *Cdkn2a* tended to increase at 20 hours; however, this increase was not significant (Fig. 1A). Furthermore, NMDA injection had no effect on the expression *Six6*, known as a Cdkn2a upstream gene (Fig. 1A).[26] *Cdkn2a* and *Cdkn2b* mRNA expression also was analyzed using ISH. Weak ISH signals for *Cdkn2a* were detected in $Rbpms^+$ RGCs, but not other cells, at 10 and 20 hours (Fig. 1B). *Cdkn2b* signals were detected in RGCs at 10 hours, and the signal intensity was substantially increased at 20 hours. *Cdkn2b* expression also was detected in the inner nuclear layer (INL) cells at 20 hours (Fig. 1B). No obvious signals for *Cdkn2a* and *Cdkn2b* were detected in any layer of PBS-injected control retinas (Fig. 1B).

Overexpression of *Cdkn2a* or *Cdkn2b* Does Not Affect RGC Survival in Healthy Mice

We next performed *Cdkn2a* and *Cdkn2b* gain-of-function experiments to investigate their role in RGC death induction using AAV2-mediated gene transfer. The AAV2 vectors contained CMV promoter-driven expression cassettes for mouse *Cdkn2a* or *Cdkn2b* tagged with the HA epitope, followed by IRES and GFP sequences (AAV2-Cdkn2a-IRES-GFP or AAV2-Cdkn2b-IRES-GFP; Fig. 2A). AAV2-IRES-GFP vector was used as a negative control. qRT-PCR analysis confirmed that the expression of both genes was drastically increased on the 32nd day after infection compared to the levels in control retinas (Fig. 2B). Unexpectedly, overexpression of *Cdkn2b* also led to increased *Cdkn2a* expression, but not vice versa (Fig. 2B). We next performed ISH and immunohistochemical analysis on retinal sections prepared from mice on the 32nd day following intravitreal injection of AAV2-Cdkn2a-IRES-GFP or AAV2-Cdkn2b-IRES-GFP, to confirm exogenous *Cdkn2a* and *Cdkn2b* expression. ISH detected abundant *Cdkn2a* and *Cdkn2b* mRNAs in $Rbpms^+$ RGCs and INL cells (Fig. 2C). Cells coexpressing GFP and Cdkn2a or Cdkn2b were detectable in the GCL of retinas injected with AAV2-Cdkn2a-IRES-GFP or AAV2-Cdkn2b-IRES-GFP, but not AAV2-IRES-GFP (Fig. 2D). This indicated that protein expression levels of endogenous Cdkn2a and Cdkn2b probably are less than the limit of detection in the normal retina, consistent with ISH data. Furthermore, double-staining of Cdkn2b immunohistochemistry and *Cdkn2a* ISH indicated that AAV2-mediated Cdkn2b overexpression resulted in upregulated *Cdkn2a* expression in the GCL (Fig. 2E), as suggested by qRT-PCR analysis. We next quantified Rbpms-immunoreactive RGCs in flat-mounted retinas prepared from mice on days 16, 24, and 32 following AAV2 infection. No significant differences were observed in the number of $Rbpms^+$ RGCs among AAV2-Cdkn2a-IRES-GFP-, AAV2-Cdkn2b-IRES-GFP-, and AAV2-IRES-GFP-infected retinas at all time points investigated (Figs. 2F, 2G).

Overexpression of *Cdkn2b*, But Not *Cdkn2a*, Increases the Susceptibility of RGCs to NMDA-Induced Death

We explored the possibility that *Cdkn2a* and *Cdkn2b* are implicated in RGC death under the pathologic condition induced by intravitreal NMDA injection. To this end, we first monitored the number of $Rbpms^+$ RGCs following NMDA injection. The

Investigative Ophthalmology & Visual Science

Downloaded from abstracts.iovs.org on 04/23/2024

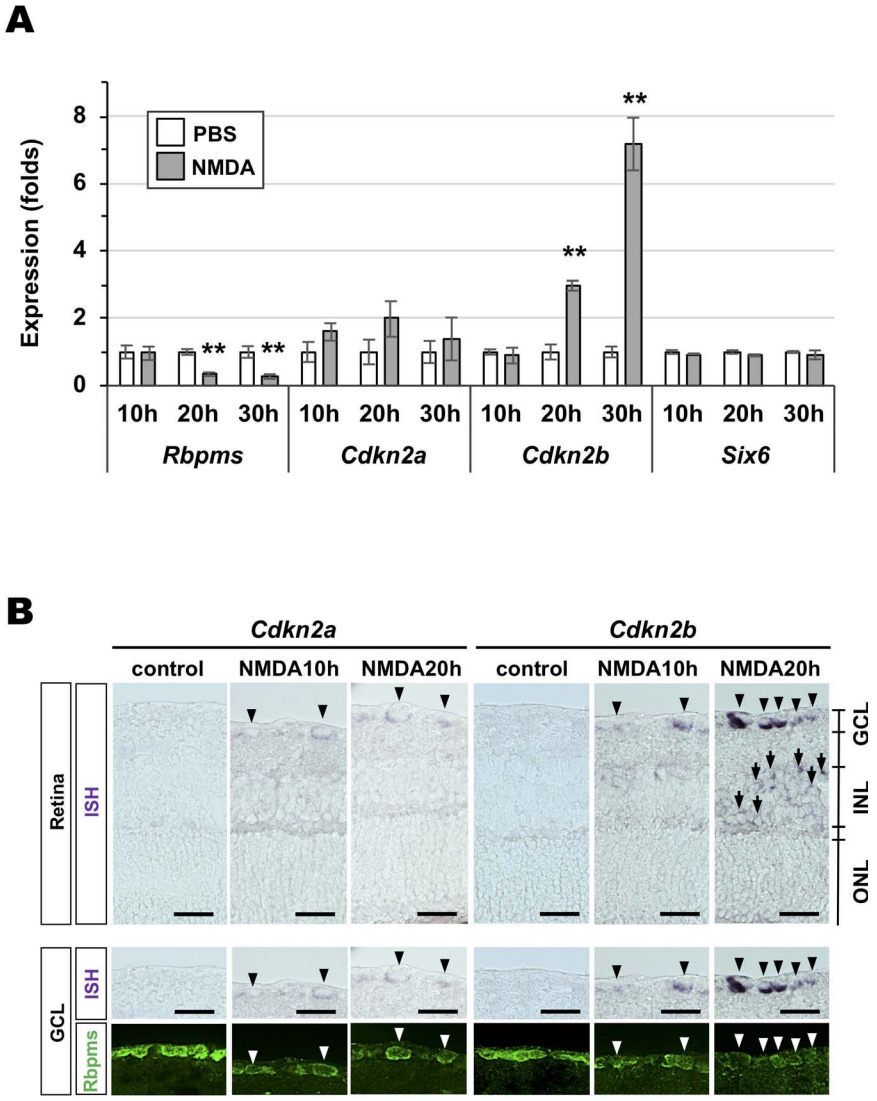

Figure 1. Gene expression changes in mouse retinas after intravitreal NMDA injection. (**A**) mRNA expression profiles of *Cdkn2a*, *Cdkn2b*, *Six6*, and *Rbpms* determined by qRT-PCR. Gene expression levels in NMDA-injected retinas are shown as a percentage of the control. *Error bars*: SEM. $^{**}P < 0.01$ vs. PBS (Student's *t*-test; $n = 5$–8). (**B**) ISH analysis of *Cdkn2a* and *Cdkn2b*, and double-staining with Rbpms immunohistochemistry. Localization of *Cdkn2a* and *Cdkn2b* mRNAs was examined on retinal sections prepared from eyes untreated (control) and treated with NMDA for 10 and 20 hours (NMDA10h and NMDA20h, upper column). The GCL is focused on in the lower column. *Cdkn2a* and *Cdkn2b* mRNAs can be detected in Rbpms^{+} RGCs. *Arrowheads* indicate RGCs coexpressing Rbpms and *Cdkn2a* or *Cdkn2b*. *Arrows* indicate INL cells expressing *Cdkn2b*. *Scale bars*: 50 μm.

number of surviving Rbpms^{+} RGCs decreased significantly at the first time point; that is, 5 hours after NMDA injection, and further decreased at 10 and 15 hours after injection (Fig. 3A). We then examined the effects of AAV2-mediated overexpression of *Cdkn2a* or *Cdkn2b* on the survival of RGCs in the retinas 10 hours after NMDA injection using Rbpms immunohistochemistry. Fewer RGCs survived in the retinas infected with AAV2-Cdkn2b-IRES-GFP, but not AAV2-Cdkn2a-IRES-GFP, than in the retinas infected with AAV2-IRES-GFP (Figs. 3B, 3C). Taken together, these results indicated that *Cdkn2b* increases the susceptibility of RGCs to NMDA-induced death.

In Vitro Validation of CRISPR-Cas9-Mediated *Cdkn2a* and *Cdkn2b* Knockout

To perform loss-of-function experiments of Cdkn2a and Cdkn2b, the CRISPR-Cas9 system consisting of *Staphylococcus aureus*-derived Cas9 and a sgRNA was used in this study (Fig. 4A). We first verified the effectiveness and accuracy of genome editing by the sgRNAs designed in the first exons of *Cdkn2a* (sgCdkn2a) and *Cdkn2b* (sgCdkn2b), and containing the translation start site, using an established mouse cell line NIH3T3-L1 (Fig. 4B). A T7E1 assay indicated successful editing of the genome of NIH3T3-L1 cells transfected with CRISPR-Cas9 plasmids encoding sgCdkn2a (CRISPR-Cas9-sgCdkn2a) or sgCdkn2b (CRISPR-Cas9-sgCdkn2b, Fig. 4C). We further investigated on- and off-target sequences of sgCdkn2a and sgCdkn2b in the genomes extracted from single-cell clones of the CRISPR-Cas9 transfectants. On-target genome editing was verified in three of 21 and 26 clones of CRISPR-Cas9-sgCdkn2a and CRISPR-Cas9-sgCdkn2b transfectants, respectively. The on-target editing effect was a deletion of several nucleotides leading to a frame shift mutation (Fig. 4D). Western blot analysis confirmed that no intact Cdkn2a and Cdkn2b proteins were detectable in each of three clones of CRISPR-Cas9-sgCdkn2a and CRISPR-cas9-

Investigative Ophthalmology & Visual Science

Downloaded from abstracts.iovs.org on 04/23/2024

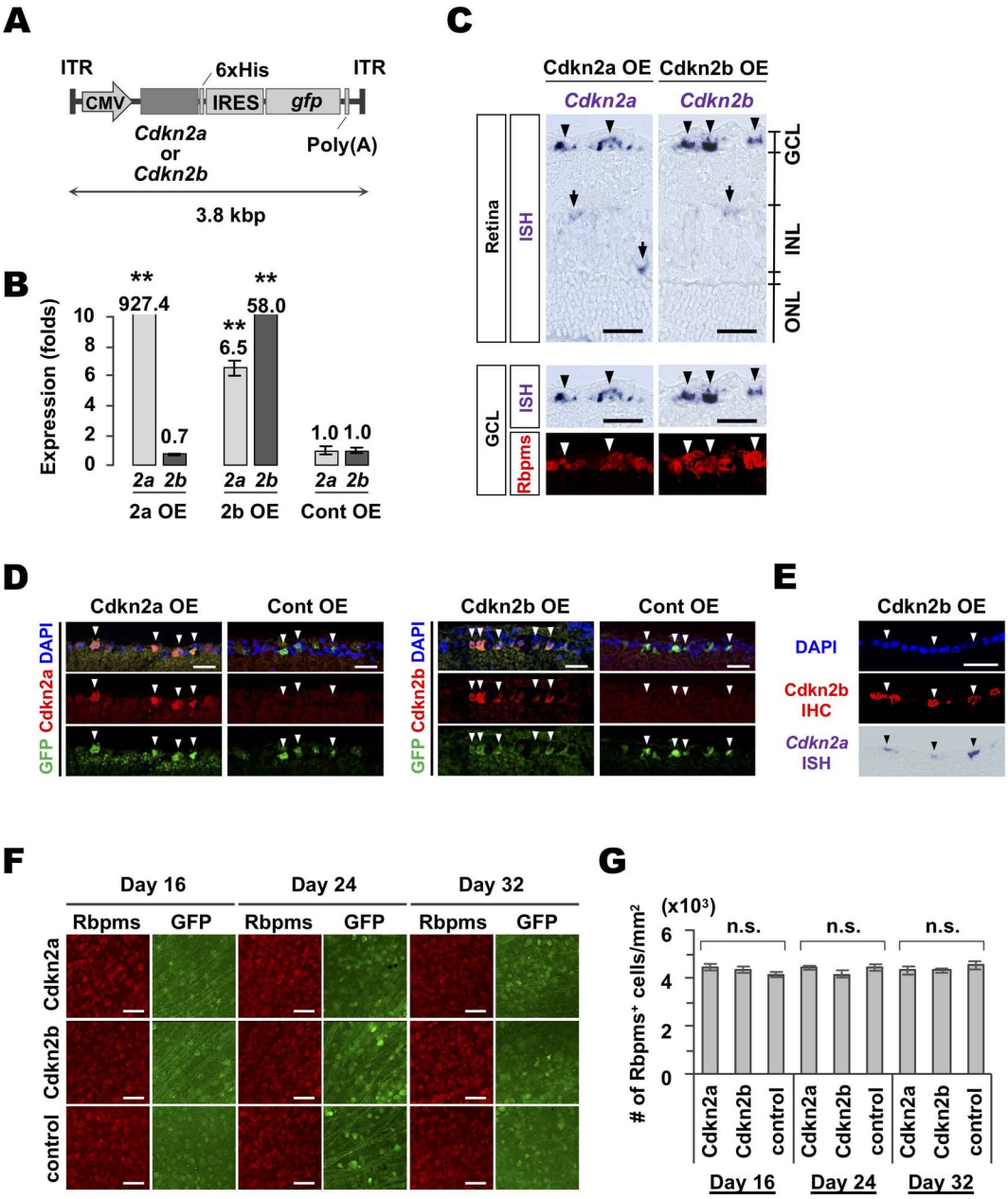

Figure 2. Effects of AAV2-mediated overexpression of *Cdkn2a* or *Cdkn2b* on RGC survival in healthy mice. (**A**) Schematic representation of the AAV2 vectors encoding Cdkn2a or Cdkn2b and GFP (AAV2-Cdkn2a-IRES-GFP or AAV2-Cdkn2b-IRES-GFP) used for gain-of-function experiments. (**B**) Upregulated expression of *Cdkn2a* and *Cdkn2b* in the retina on day 32 after AAV2 infection determined by qRT-PCR. The number above each *bar* indicates the actual relative fold change in the expression level compared to the control. Note that infection of the AAV2 vectors expressing *Cdkn2b* significantly increased the expression levels of *Cdkn2b* and *Cdkn2a*. (**C**) ISH analysis of *Cdkn2a* and *Cdkn2b*, and double-staining with Rbpms immunohistochemistry. Localization of *Cdkn2a* and *Cdkn2b* mRNAs was examined on retinal sections prepared from eyes infected with AAV2-Cdkn2a-IRES-GFP or AAV2-Cdkn2b-IRES-GFP (*upper column*). The GCL is focused on in the *lower column*. *Arrowheads* and *arrows* indicate *Cdkn2a*- or *Cdkn2b*-expressing Rbpms^{+} RGCs and INL cells, respectively. (**D**) Expression of Cdkn2a and Cdkn2b proteins on day 32 after AAV2 infection according to immunohistochemistry. Protein localization of exogenous or endogenous Cdkn2a (*left*) and Cdkn2b proteins (*right*) is shown in the GCL of retinas infected with AAV2-Cdkn2a-IRES-GFP or AAV2-Cdkn2b-IRES-GFP, and AAV2-IRES-GFP. *Arrowheads* indicate AAV2-infected cells coexpressing exogenous Cdkn2a or Cdkn2b and GFP. Note that the expression level of endogenous Cdkn2a and Cdkn2b is below the detection limit. (**E**) Double-staining of Cdkn2b immunohistochemistry and *Cdkn2a* ISH. *Cdkn2a* mRNA localization was examined in the GCL of the retina on day 32 after AAV2-Cdkn2b-IRES-GFP infection. Cdkn2b-overexpressing GCL cells co-express *Cdkn2a* (*arrowheads*). (**F**) Immunostaining of the RGC marker Rbpms and GFP in the retina on days 16, 24, and 32 after AAV2 infection. (**G**) Quantification of Rbpms^{+} RGCs in AAV2-injected retinas. *Error bars*: SEM. n.s., not significant. $^{**}P < 0.01$ versus control (Tukey-Kramer test; $n = 6$ in [**B**] and 5–9 in [**G**]). *Scale bar*: 50 µm.

sgCdkn2b transfectants (Fig. 4E). Off-target sites for sgCdkn2a and sgCdkn2b, as predicted in silico (CRISPOR; available in the public domain at http://crispor.tefor.net/; Supplementary Table S4), had no detectable modification in these clones.

Loss of Cdkn2a or Cdkn2b Attenuates NMDA-Induced RGC Death

Intravitreal injection of AAV2 vectors encoding CRISPR-Cas9 and sgRNA into the mouse retina led to successful expression

Investigative Ophthalmology & Visual Science

Downloaded from abstracts.iovs.org on 04/23/2024

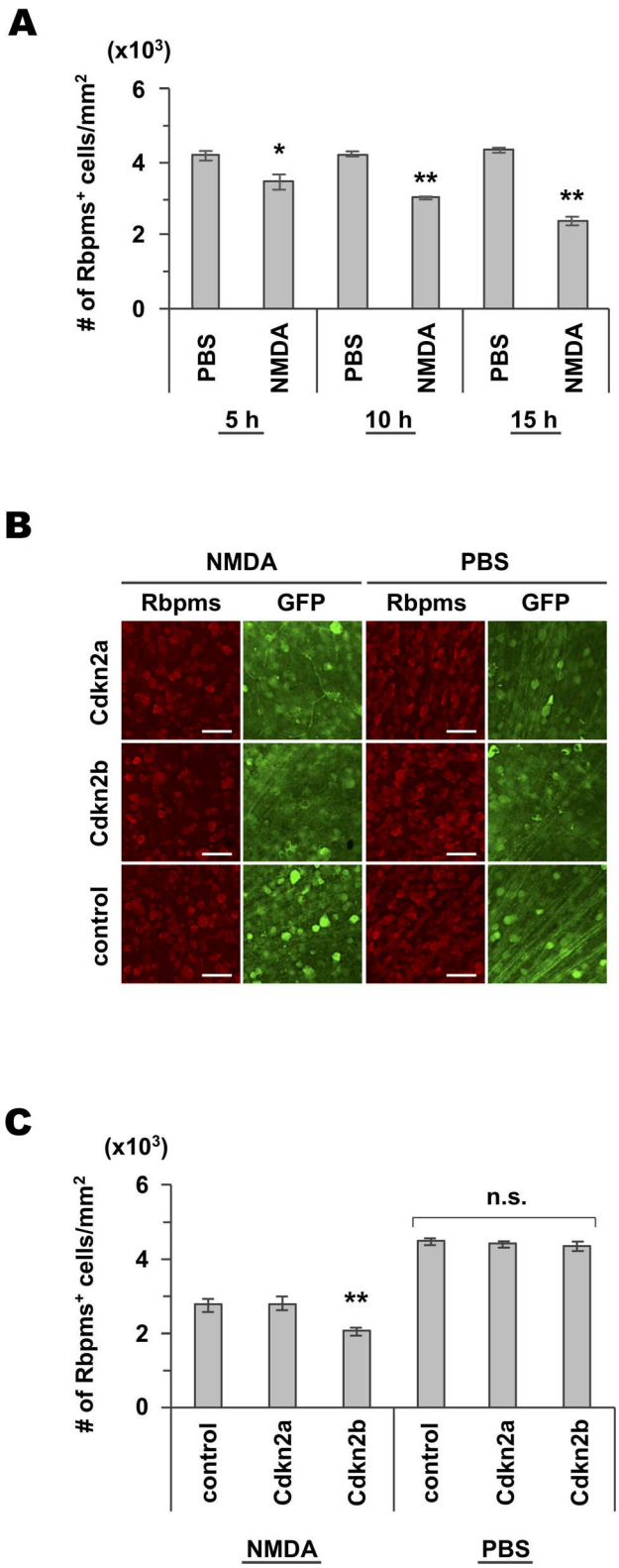

Figure 3. Effect of AAV2-mediated overexpression of *Cdkn2a* or *Cdkn2b* on RGC survival in NMDA-injected mice. (**A**) Time-course changes in the number of Rbpms$^+$ RGCs following intravitreal injection of NMDA (10 nmol). (**B**) Immunostaining for the RGC marker Rbpms and GFP in flat-mounted retinas infected with AAV2-Cdkn2a-IRES-GFP or AAV2-Cdkn2b-IRES-GFP. (**C**) Quantification of Rbpms$^+$ RGCs in AAV2-infected retinas after NMDA injection. A decrease in the number of Rbpms$^+$ RGCs was observed upon overexpression of *Cdkn2b*, but not *Cdkn2a*. *Error bars*: SEM. $^*P < 0.05$, $^{**}P < 0.01$ versus control (Student's *t*-test and Tukey-Kramer test; $n = 5$ and 5–6 in [**A**] and [**C**], respectively). *Scale bar*: 50 μm.

of Cas9 proteins in RGCs in our previous study.[36] In our study, AAV2 vectors encoding CRISPR-Cas9-sgCdkn2a (AAV2-Cas9-sgCdkn2a) or CRISPR-Cas9-sgCdkn2b (AAV2-Cas9-sgCdkn2b), and AAV2-IRES-GFP as an infection control, were coinjected intravitreally to knockout *Cdkn2a* or *Cdkn2b* in RGCs in vivo. NMDA was intravitreally administered on the day 32 following virus injection to examine the effect of loss of Cdkn2a or Cdkn2b on NMDA-induced RGC death (Fig. 5A). Loss of Cdkn2a or Cdkn2b significantly prevented NMDA-induced cell death in Rbpms$^+$ RGCs compared to control cells infected with nonsense sgRNA-encoding AAV2 (Fig. 5B). Furthermore, a higher number of RGCs was observed in the retinas deficient for Cdkn2b than in those deficient for Cdkn2a.

Discussion

In our study, we characterized the phenotypic changes in NMDA-induced RGC death in mouse retinas, in which either *Cdkn2a* or *Cdkn2b* was overexpressed or knocked out using AAV2-mediated transgene expression. Results showed that loss of Cdkn2a or Cdkn2b attenuated NMDA-induced cell death in RGCs; moreover, Cdkn2b overexpression enhanced NMDA-induced RGC death. Intravitreal AAV2 injection induced transgene expression under control of the CMV promoter in RGCs as well as in other retinal cells.[38–40] We believe that the phenotypic changes observed in AAV2-infected retinas could be attributed primarily to altered expression of Cdkn2a or Cdkn2b in RGCs, as shown by the following results. First, a higher infection efficiency was found in RGCs than in other cell types in AAV2-infected retinas (Supplementary Fig. S1). Second, endogenous Cdkn2a and Cdkn2b expression was undetectable in the retinas of the control group, but markedly upregulated in RGCs in response to NMDA (Fig. 1B). Finally, NMDA-induced RGC death could occur due to a direct effect of NMDA on RGCs. Previous studies have reported that retinal cells, such as amacrine, bipolar, and horizontal cells, as well as RGCs express NMDA receptor subunits, and are potentially sensitive to NMDA.[38–40] Thus, NMDA-mediated loss of the retinal cells, other than RGCs, could induce RGC death as its secondary effect. However, intravitreal NMDA injection increased the number of TUNEL$^+$ cells in the GCL earlier than in the INL and outer nuclear layer (ONL; Supplementary Fig. S2); most of the TUNEL$^+$ cells in the GCL were Rbpms-expressing RGCs (92.1%; Supplementary Fig. S2). Taken together, we concluded that attenuation and enhancement of RGC death in AAV2-infected retinas were due to the primary effect of altered expression of Cdkn2a and Cdkn2b in RGCs.

Expression of Cdkn2a and Cdkn2b was altered in experimental animal models of glaucoma and ischemia-reperfusion injury, and Cdkn2a deficiency results in attenuation of cell death.[26,30,32,41] However, the molecular mechanism underlying Cdkn2a-mediated cell death has not been completely elucidated. Cdkn2a can form a molecular complex with Cdk4 and the tumor suppressor p53, enhancing the binding efficiency of p53 to the promoter region of its target genes related to cell cycling and apoptosis.[42] Thus, proapoptotic genes, such as *Bax*, *p63*, and *p73*, were downregulated following knockout of Cdkn2a.[42] Another study demonstrated that overexpression of p53 and Cdkn2a, but not p53 alone, triggered apoptosis in tumor cells.[43] Given that NMDA-induced RGC death is partially mediated by p53,[44] the prevention of RGC death following Cdkn2a knockout observed in our study may be attributable, at least in part, to attenuation of p53 signaling. In contrast to Cdkn2a, little is known about the molecular mechanism underlying Cdkn2b-mediated cell death induction. Cdkn2b has similar binding properties as Cdkn2a in terms of interacting with common members of the cyclin-dependent kinase family

Investigative Ophthalmology & Visual Science

Downloaded from abstracts.iovs.org on 04/23/2024

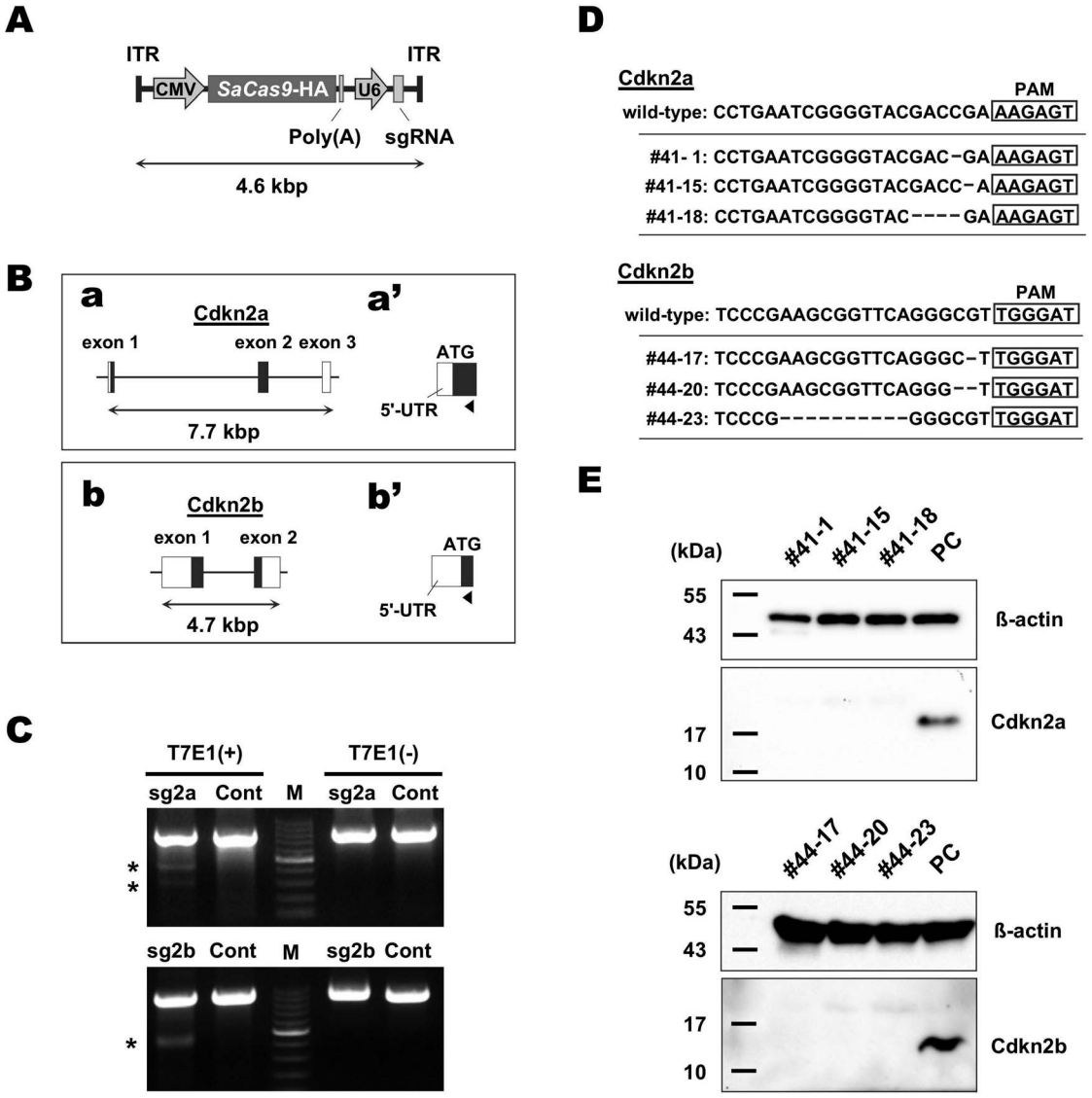

FIGURE 4. In vitro validation of CRISPR-Cas9-mediated knockout of *Cdkn2a* and *Cdkn2b*. (**A**) Schematic representation of the AAV-CRISPR-Cas9 construct. (**B**) The location of CRISPR-Cas9 targets. The entire genome structures of the *Cdkn2a* and *Cdkn2b* genes are shown in (**a**) and (**b**), respectively. The first exons of *Cdkn2a* and *Cdkn2b* in (**a**) and (**b**) are magnified in (**a'**) and (**b'**), respectively. *Black triangles* in (**a'**) and (**b'**) indicate the locations of CRISPR-Cas9 on-targets on exon 1 of each gene (see Materials and Methods for details). *White* and *gray boxes* indicate untranslated and coding regions, respectively. (**C**) Genome editing effects of CRISPR-Cas9-sgCdkn2a (sg2a), CRISPR-Cas9-sgCdkn2b (sg2b), and CRISPR-Cas9 control (Cont) in NIH3T3-L1 cells. A T7E1 assay was performed on FACS-sorted bulk transfectants of CRISPR-Cas9 plasmids. *Asterisks* indicate T7E1-mediated digestion of PCR amplicons. M: 100-bp DNA ladder. (**D**) Modification of the target sequences of CRISPR-Cas9-sgCdkn2a (upper) and CRISPR-Cas9-sgCdkn2b (lower) in each of three FACS-sorted clones obtained from plasmid transfectants. (**E**) Immunochemical detection of endogenous Cdkn2a (upper) or Cdkn2b (lower), with β-actin as an internal control in the same clones as described in (**D**). UTR, untranslated region; PC, parental cell.

(i.e., CDK4 and 6).[17–19] Therefore, it is possible that Cdkn2b induces RGC death via a molecular mechanism similar to that of Cdkn2a.

Cdkn2a and Cdkn2b have been shown previously to exert identical effects on tumor cells, such as inhibition of cell growth and telomerase activity, and senescence induction.[45] Our study indicated that knockout of either *Cdkn2a* or *Cdkn2b* rescued NMDA-induced RGC loss, suggesting their similar roles in the context of RGC death induction. However, this study also revealed potential differences in physiologic functions between Cdkn2a and Cdkn2b: knockout of Cdkn2b resulted in stronger inhibition of NMDA-induced RGC death than did knockout of Cdkn2a. This phenomenon can be explained partially by the novel finding that Cdkn2b can stimulate Cdkn2a expression, but not vice versa. CRISPR-Cas9-mediated knockout of Cdkn2b led to a reduction in not only Cdkn2b, but also Cdkn2a proteins in RGCs. Thus, Cdkn2b knockout would be more effective in preventing NMDA-induced RGC loss. Another striking difference between Cdkn2a and Cdkn2b is that overexpression of Cdkn2b facilitated RGC loss in NMDA-treated retinas, whereas overexpression of Cdkn2a did not. Endogenous Cdkn2b expression was upregulated gradually in RGCs after NMDA injection, coincident with an increase in RGC death (Fig. 1B). This implies that there is a critical correlation between Cdkn2b expression and NMDA-mediated RGC death. In contrast, Cdkn2a expression increased in response to NMDA; however, its expression level did not increase over time (Figs. 1A, 1B).

Investigative Ophthalmology & Visual Science

Downloaded from abstracts.iovs.org on 04/23/2024

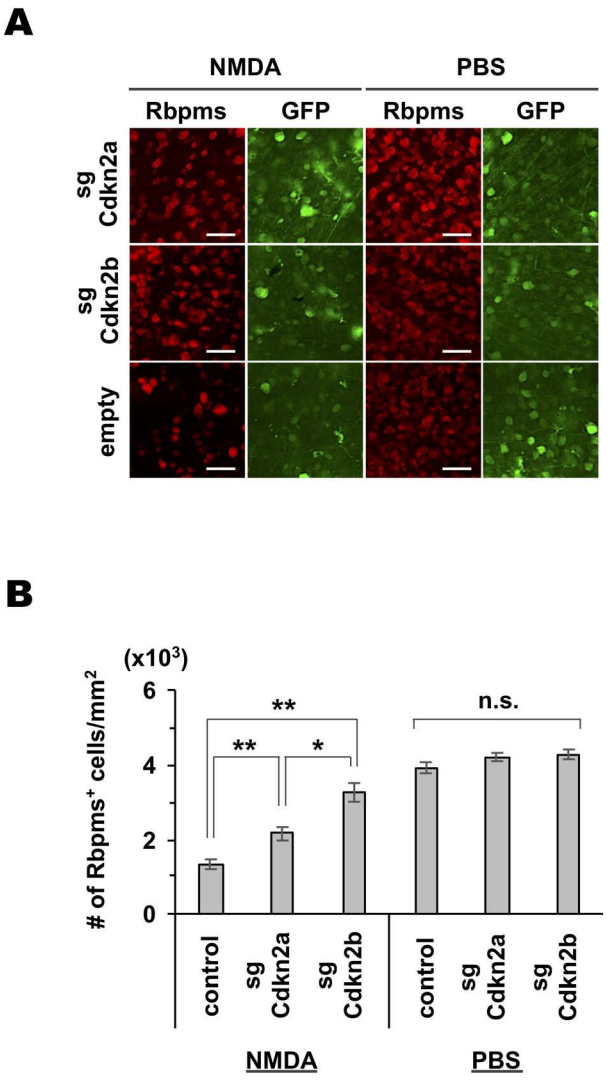

FIGURE 5. Impact of CRISPR-Cas9-mediated loss of Cdkn2a or Cdkn2b on NMDA-induced RGC reduction. (**A**) Immunostaining for Rbpms and GFP in NMDA-treated retinas co-infected with AAV2 vectors containing the *SaCas9* gene and an sgRNA sequence (AAV2-SaCas9-sgRNA), or containing the *gfp* gene, as an infection control (AAV2-GFP). (**B**) Quantification of $Rbpms^+$ RGCs in AAV2-injected retinas after NMDA injection. The number of surviving RGCs increased when *Cdkn2a* or *Cdkn2b* was knocked out. *Error bars*: SEM. $^*P < 0.05$, $^{**}P < 0.01$ (Tukey-Kramer test; $n = 5$–8). *Scale bar*: 50 μm.

Because Cdkn2a expression was undetectable in the control retinas untreated with NMDA, the role of Cdkn2a in NMDA-induced RGC death may depend on the presence of Cdkn2a, but be independent of its expression level. Taken together, we hypothesized that Cdkn2b has the ability to facilitate NMDA-induced RGC death by coexistence with Cdkn2a. Thus, the loss of either Cdkn2a or Cdkn2b can attenuate RGC death in NMDA-treated retinas.

Intravitreal NMDA administration results in RGC degeneration due to neuronal excitotoxicity.[33,34] The degeneration process would be triggered by excessive influx of extracellular calcium into cells via NMDA-type glutamate receptors.[46–48] Calcium accumulation hyperactivates intracellular enzymes, including proteases, kinases, phospholipases, and neuronal nitric oxide synthase, leading to oxidative stress.[49–57] Oxidative stress-induced cellular damage drives senescence, coincident with increased expression of senescence markers, such as SA-ß-gal, Cdkn2a, and Cdkn2b.[58,59] Consistent with these, increased expression of senescence markers Cdkn2a and Cdkn2b was observed in RGCs suffering NMDA-mediated oxidative stress. Cellular senescence is found initially as a unique state of normal mitotic cells displaying the limited replicative property after repeated proliferation.[60] Accumulating evidence has indicated that differentiated postmitotic neurons as well as normal mitotic cells show senescence-like state, characteristic of senescence marker expression, with age, and also in response to various cellular stresses and damages.[61] This could lead to pathogenesis of senescence-related diseases.[59] In an animal model of glaucoma, high IOP induced upregulated expression of Six6 and Cdkn2a, and genetic reduction of Six6 and Cdkn2a led to decreased expression of Cdkn2a and rescue of the RGC loss phenotype, respectively.[26] On the other hand, our study indicated that NMDA-induced excitotoxity upregulated the expression of Cdkn2a and Cdkn2b, but not Six6. Considering these findings, expression of senescence genes, such as *Cdkn2a* and *Cdkn2b*, appears to be triggered in response to different extrinsic and intrinsic stresses, suggesting that these proteins function as downstream cell death signal transducers.

In conclusion, we elucidated the roles of Cdkn2a and Cdkn2b in RGCs using in vivo gain- and loss-of-function approaches, and found that these molecules, especially Cdkn2b, are essential for NMDA-induced cell death. Our results suggested that Cdkn2a and Cdkn2b are potential therapeutic targets to prevent RGC degeneration observed in eye diseases related to neuronal excitotoxicity, including ischemia-reperfusion injury and glaucoma.

Acknowledgements

The authors thank Junko Sato and Mayumi Suda for technical assistance, and the Biomedical Research Unit of Tohoku University Hospital for technical support.

Supported by JSPS KAKENHI Grant Number JP17H04349 (T.N.) from the Ministry of Education, Science and Technology of Japan.

Disclosure: **H. Tawarayama**, None; **Q. Feng**, None; **N. Murayama**, None; **N. Suzuki**, None; **T. Nakazawa**, None

References

1. Casson RJ. Possible role of excitotoxicity in the pathogenesis of glaucoma. *Clin Exp Ophthalmol*. 2006;34:54–63.
2. Kaur C, Foulds WS, Ling E-A. Hypoxia-ischemia and retinal ganglion cell damage. *Clin Ophthalmol*. 2008;2:879–889.
3. Hernández C, Simó R. Neuroprotection in diabetic retinopathy. *Curr Diab Rep*. 2012;12:329–337.
4. Harada T, Harada C, Nakamura K, et al. The potential role of glutamate transporters in the pathogenesis of normal tension glaucoma. *J Clin Invest*. 2007;117:1763–1770.
5. Maekawa S, Sato K, Fujita K, et al. The neuroprotective effect of hesperidin in NMDA-induced retinal injury acts by suppressing oxidative stress and excessive calpain activation. *Sci Rep*. 2017;7:6885.
6. Nakazawa T, Shimura M, Endo S, Takahashi H, Mori N, Tamai M. N-Methyl-D-Aspartic acid suppresses Akt activity through protein phosphatase in retinal ganglion cells. *Mol Vis*. 2005; 11:1173–1182.
7. Nakazawa T, Takahashi H, Nishijima K, et al. Pitavastatin prevents NMDA-induced retinal ganglion cell death by suppressing leukocyte recruitment. *J Neurochem*. 2007;100: 1018–1031.
8. Nakazawa T, Watanabe M, Kudo H, Nishida K, Tamai M. Susceptibility to N-methyl-D-aspartate toxicity in morpholog-

Investigative Ophthalmology & Visual Science

Downloaded from abstracts.iovs.org on 04/23/2024

ical and functional types of cat retinal ganglion cells. *Jpn J Ophthalmol*. 2010;54:156–162.

9. Toriu N, Akaike A, Yasuyoshi H, et al. Lomerizine, a Ca2+ channel blocker, reduces glutamate-induced neurotoxicity and ischemia/reperfusion damage in rat retina. *Exp Eye Res*. 2000;70:475–484.
10. Adachi K, Kashii S, Masai H, et al. Mechanism of the pathogenesis of glutamate neurotoxicity in retinal ischemia. *Graefes Arch Clin Exp Ophthalmol*. 1998;236:766–774.
11. Adachi M, Takahashi K, Nishikawa M, Miki H, Uyama M. High intraocular pressure-induced ischemia and reperfusion injury in the optic nerve and retina in rats. *Graefes Arch Clin Exp Ophthalmol*. 1996;234:445–451.
12. Osborne NN, DeSantis L, Bae JH, et al. Topically applied betaxolol attenuates NMDA-induced toxicity to ganglion cells and the effects of ischaemia to the retina. *Exp Eye Res*. 1999; 69:331–342.
13. Osborne NN. Memantine reduces alterations to the mammalian retina, in situ, induced by ischemia. *Vis Neurosci*. 1999; 16:45–52.
14. Bai N, Aida T, Yanagisawa M, et al. NMDA receptor subunits have different roles in NMDA-induced neurotoxicity in the retina. *Mol Brain*. 2013;6:34.
15. Lagrèze WA, Knörle R, Bach M, Feuerstein TJ. Memantine is neuroprotective in a rat model of pressure-induced retinal ischemia. *Invest Ophthalmol Vis Sci*. 1998;39:1063–1066.
16. Schuettauf F, Quinto K, Naskar R, Zurakowski D. Effects of anti-glaucoma medications on ganglion cell survival: the DBA/2J mouse model. *Vision Res*. 2002;42:2333–2337.
17. Serrano M, Hannon GJ, Beach D. A new regulatory motif in cell-cycle control causing specific inhibition of cyclin D/CDK4. *Nature*. 1993;366:704–707.
18. Guan KL, Jenkins CW, Li Y, et al. Growth suppression by p18, a p16INK4/MTS1- and p14INK4B/MTS2-related CDK6 inhibitor, correlates with wild-type pRb function. *Genes Dev*. 1994; 8:2939–2952.
19. Koh J, Enders GH, Dynlacht BD, Harlow E. Tumour-derived p16 alleles encoding proteins defective in cell-cycle inhibition. *Nature*. 1995;375:506–510.
20. Sherr CJ. G1 phase progression: cycling on cue. *Cell*. 1994;79: 551–555.
21. Sherr CJ. Mammalian G1 cyclins. *Cell*. 1993;73:1059–1065.
22. Agiostratidou G, Derventzi A, Gonos ES. Over-expression of CDKIs p15INK4b, p16INK4a and p21CIP1/WAF1 genes mediate growth arrest in human osteosarcoma cell lines. *In Vivo*. 2001;15:443–446.
23. Krishnamurthy J, Torrice C, Ramsey MR, et al. Ink4a/Arf expression is a biomarker of aging. *J Clin Invest*. 2004;114: 1299–1307.
24. Campisi J. Aging, cellular senescence, and cancer. *Annu Rev Physiol*. 2013;75:685–705.
25. Naylor RM, Baker DJ, van Deursen JM. Senescent cells: a novel therapeutic target for aging and age-related diseases. *Clin Pharmacol Ther*. 2013;93:105–116.
26. Skowronska-Krawczyk D, Zhao L, Zhu J, et al. P16INK4a Upregulation mediated by SIX6 defines retinal ganglion cell pathogenesis in glaucoma. *Mol Cell*. 2015;59:931–940.
27. Vidal-Sanz M, Salinas-Navarro M, Nadal-Nicolás FM, et al. Understanding glaucomatous damage: anatomical and functional data from ocular hypertensive rodent retinas. *Prog Retin Eye Res*. 2012;31:1–27.
28. Congrains A, Kamide K, Ohishi M, Rakugi H. ANRIL: molecular mechanisms and implications in human health. *Int J Mol Sci*. 2013;14:1278–1292.
29. Burdon KP, Crawford A, Casson RJ, et al. Glaucoma risk alleles at CDKN2B-AS1 are associated with lower intraocular pressure, normal-tension glaucoma, and advanced glaucoma. *Ophthalmology*. 2012;119:1539–1545.
30. Burdon KP, Macgregor S, Hewitt AW, et al. Genome-wide association study identifies susceptibility loci for open angle glaucoma at TMCO1 and CDKN2B-AS1. *Nat Genet*. 2011;43: 574–578.
31. Shiga Y, Nishiguchi KM, Kawai Y, et al. Genetic analysis of Japanese primary open-angle glaucoma patients and clinical characterization of risk alleles near CDKN2B-AS1, SIX6 and GAS7. *PLoS One*. 2017;12:e0186678.
32. Gao S, Jakobs TC. Mice Homozygous for a deletion in the glaucoma susceptibility locus INK4 show increased vulnerability of retinal ganglion cells to elevated intraocular pressure. *Am J Pathol*. 2016;186:985–1005.
33. Li Y, Schlamp CL, Nickells RW. Experimental induction of retinal ganglion cell death in adult mice. *Invest Ophthalmol Vis Sci*. 1999;40:1004–1008.
34. Lam TT, Abler AS, Kwong JM, Tso MO. N-methyl-D-aspartate (NMDA)–induced apoptosis in rat retina. *Invest Ophthalmol Vis Sci*. 1999;40:2391–2397.
35. Ran FA, Cong L, Yan WX, et al. In vivo genome editing using Staphylococcus aureus Cas9. *Nature*. 2015;520:186–191.
36. Sato K, Shiga Y, Nakagawa Y, et al. Ecel1 knockdown with an AAV2-mediated CRISPR/Cas9 system promotes optic nerve damage-induced RGC death in the mouse retina. *Invest Ophthalmol Vis Sci*. 2018;59:3943–3951.
37. Tawarayama H, Yoshida Y, Suto F, Mitchell KJ, Fujisawa H. Roles of semaphorin-6B and plexin-A2 in lamina-restricted projection of hippocampal mossy fibers. *J Neurosci*. 2010;30: 7049–7060.
38. Harvey AR, Kamphuis W, Eggers R, et al. Intravitreal injection of adeno-associated viral vectors results in the transduction of different types of retinal neurons in neonatal and adult rats: a comparison with lentiviral vectors. *Mol Cell Neurosci*. 2002; 21:141–157.
39. Hellström M, Ruitenberg MJ, Pollett MA, et al. Cellular tropism and transduction properties of seven adeno-associated viral vector serotypes in adult retina after intravitreal injection. *Gene Ther*. 2009;16:521–532.
40. Hori T, Fukutome M, Koike C. Adeno Associated Virus (AAV) as a Tool for Clinical and Experimental Delivery of Target Genes into the Mammalian Retina. *Biol Pharm Bull*. 2019;42: 343–347.
41. Lee DH, Wolstein JM, Pudasaini B, Plotkin M. INK4a deletion results in improved kidney regeneration and decreased capillary rarefaction after ischemia-reperfusion injury. *Am J Physiol Renal Physiol*. 2012;302:F183–F191.
42. Al-Khalaf HH, Nallar SC, Kalvakolanu DV, Aboussekhra A. p16INK4A enhances the transcriptional and the apoptotic functions of p53 through DNA-dependent interaction. *Mol Carcinog*. 2017;56:1687–1702.
43. Sandig V, Brand K, Herwig S, Lukas J, Bartek J, Strauss M. Adenovirally transferred p16INK4/CDKN2 and p53 genes cooperate to induce apoptotic tumor cell death. *Nat Med*. 1997;3:313–319.
44. Li Y, Schlamp CL, Poulsen GL, Jackson MW, Griep AE, Nickells RW. p53 regulates apoptotic retinal ganglion cell death induced by N-methyl-D-aspartate. *Mol Vis*. 2002;8:341–350.
45. Fuxe J, Akusjärvi G, Goike HM, Roos G, Collins VP, Pettersson RF. Adenovirus-mediated overexpression of p15INK4B inhibits human glioma cell growth, induces replicative senescence, and inhibits telomerase activity similarly to p16INK4A. *Cell Growth Differ*. 2000;11:373–384.
46. Choi DW. Ionic dependence of glutamate neurotoxicity. *J Neurosci*. 1987;7:369–379.
47. Berdichevsky E, Riveros N, Sánchez-Armáss S, Orrego F. Kainate, N-methylaspartate and other excitatory amino acids

Investigative Ophthalmology & Visual Science

Downloaded from abstracts.iovs.org on 04/23/2024

increase calcium influx into rat brain cortex cells in vitro. *Neurosci Lett*. 1983;36:75–80.

48. Choi DW. Glutamate neurotoxicity in cortical cell culture is calcium dependent. *Neurosci Lett*. 1985;58:293–297.
49. Ganapathy PS, White RE, Ha Y, et al. The role of N-methyl-D-aspartate receptor activation in homocysteine-induced death of retinal ganglion cells. *Invest Ophthalmol Vis Sci*. 2011;52:5515–5524.
50. Sattler R, Tymianski M. Molecular mechanisms of calcium-dependent excitotoxicity. *J Mol Med*. 2000;78:3–13.
51. Orrenius S, Zhivotovsky B, Nicotera P. Regulation of cell death: the calcium-apoptosis link. *Nat Rev Mol Cell Biol*. 2003;4:552–565.
52. Nakazawa T, Shimura M, Mourin R, et al. Calpain-mediated degradation of G-substrate plays a critical role in retinal excitotoxicity for amacrine cells. *J Neurosci Res*. 2009;87:1412–1423.
53. Yokoyama Y, Maruyama K, Yamamoto K, et al. The role of calpain in an in vivo model of oxidative stress-induced retinal ganglion cell damage. *Biochem Biophys Res Commun*. 2014;451:510–515.
54. Murphy MP. How mitochondria produce reactive oxygen species. *Biochem J*. 2009;417:1–13.
55. Moncada S, Bolaños JP. Nitric oxide, cell bioenergetics and neurodegeneration. *J Neurochem*. 2006;97:1676–1689.
56. Coyle JT, Puttfarcken P. Oxidative stress, glutamate, and neurodegenerative disorders. *Science*. 1993;262:689–695.
57. Choi DW. Excitotoxic cell death. *J Neurobiol*. 1992;23:1261–1276.
58. Vurusaner B, Poli G, Basaga H. Tumor suppressor genes and ROS: complex networks of interactions. *Free Radic Biol Med*. 2012;52:7–18.
59. Muñoz-Espín D, Serrano M. Cellular senescence: from physiology to pathology. *Nat Rev Mol Cell Biol*. 2014;15:482–496.
60. Hayflick L. The limited in vitro lifetime of human diploid cell strains. *Exp Cell Res*. 1965;37:614–636.
61. Sapieha P, Mallette FA. Cellular senescence in postmitotic cells: beyond growth arrest. *Trends Cell Biol*. 2018;28:595–607.

Investigative Ophthalmology & Visual Science

Downloaded from abstracts.iovs.org on 04/23/2024